Journal of Colloid and Interface Science 495 (2017) 44–52

Contents lists available at ScienceDirect

Journal of Colloid and Interface Science

journal homepage: www.elsevier.com/locate/jcis

Regular Article

Adsorbent synthesis of polypyrrole/TiO_2 for effective fluoride removal from aqueous solution for drinking water purification: Adsorbent characterization and adsorption mechanism

Jie Chen [a], Chiajung Shu [b], Ning Wang [a], Jiangtao Feng [a,*], Hongyu Ma [a], Wei Yan [a,*]

[a] State Key Laboratory of Multiphase Flow in Power Engineering, Department of Environmental Science and Engineering, Xi'an Jiaotong University, China
[b] Department of Bioenvironmental Systems Engineering, National Taiwan University, China

GRAPHICAL ABSTRACT

The PPy/TiO_2 composite can be used in the purification of fluoride containing water for drinking. The adsorption is prominently conducted through electrostatic attraction, and ionic exchange and chelation may be also involved. Hydroxyls and positively charged nitrogen atoms play important roles in the adsorption.

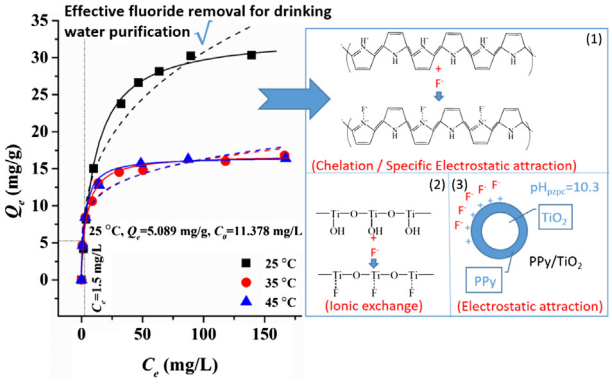

ARTICLE INFO

Article history:
Received 13 November 2016
Revised 4 January 2017
Accepted 22 January 2017
Available online 24 January 2017

Keywords:
PPy/TiO_2
Drinking water defluoridation
Adsorption behavior investigation
Adsorption mechanism

ABSTRACT

More than 20 countries are still suffering problems of excessive fluoride containing water, and greater than 8 mg/L fluoride groundwater has been reported in some villages in China. In order to meet the challenge in the drinking water defluoridation engineering, a high efficiency and affinity defluoridation adsorbent PPy/TiO_2 composite was designed and synthetized by in-situ chemical oxidative polymerization. Fourier Transform Infrared Spectroscopy (FTIR), X-ray diffraction Investigator (XRD), X-ray photoelectron spectroscopy (XPS), Thermogravimetric analysis (TG), N_2 isotherm analysis, Scanning Electron Microscopy (SEM) and Zeta potential analysis were conducted to characterize surface and textural properties of the as-prepared PPy/TiO_2, and the possibility of fluoride adsorption was carefully estimated by adsorption isotherm and kinetic studies. Characterization investigations demonstrate the uniqueness of surface and textural properties, such as suitable specific surface area and abundant positively charged nitrogen atoms (N^+), which indicate the composite is a suitable material for the fluoride adsorption. Adsorption isotherms and kinetics follow better with Langmuir and pseudo-second-order model,

* Corresponding authors.
E-mail addresses: fjtes@xjtu.edu.cn (J. Feng), yanwei@xjtu.edu.cn (W. Yan).

http://dx.doi.org/10.1016/j.jcis.2017.01.084

respectively. The maximum adsorption capacity reaches 33.178 mg/g at 25 °C according to Langmuir model, and particular interest was the ability to reduce the concentration of fluoride from 11.678 mg/L to 1.5 mg/L for drinking water at pH of 7 within 30 min. Moreover, the adsorbent can be easily recycled without the loss of adsorption capacity after six cycles, greatly highlighting its outstanding affinity to fluoride, low-cost and novel to be used in the purification of fluoride containing water for drinking. Furthermore, the adsorption mechanism was extensively investigated and discussed by FTIR investigation and batch adsorption studies including effect of pH, surface potential and thermodynamics. The adsorption is confirmed to be a spontaneous and exothermic process with decreasing entropy, which is prominently conducted through electrostatic attraction, and ionic exchange, and chelation may be also involved. Hydroxyls and positively charged nitrogen atoms play important roles in the adsorption.

1. Introduction

Fluoride is an essential element for humans and animals related to the total amount ingested [1]. The presence of fluoride has beneficial effects on the maintenance of bones and teeth at low concentrations (0.5–1.0 ppm), however various adverse problems would be risen such as teeth mottling, neurological damage, bones softening and so on within an excessive exposure [2,3]. Currently, the problem in terms of fluoride contamination of groundwater due to natural and anthropogenic activities has become one of the most concerned issues in the environment protection in the worldwide. The fluoride can be leached out by the rainwater from minerals in the wild. The fluoride is also widely used in industrial productions, such as nuclear, aluminum industries, semiconductors and fertilizer applications, resulting in a large amount of fluoride containing wastewater [1]. The maximum fluoride allowable concentration in drinking water set by World Health Organization (WHO) is 1.5 mg/L [4]. However, more than 20 countries are still suffering fluorosis problems of excessive fluoride containing water [5,6], and greater than 8 mg/L fluoride groundwater has been reported in some villages in China [7]. Thus, the fluoride containing water has become a serious topic nowadays.

Various technologies, including adsorption [8], ion exchange [9], electro-techniques [10], membrane separation [11], precipitation [12], etc. have been proposed to solve fluoride issues. Adsorption, which is simple, low-cost and economical, is extensively applied in water defluoridation applications [8]. To find an adsorbent with high adsorption capacity and fast adsorption kinetic for fluoride removal, activated carbon [13], calcite [14], activated alumina [1], rare earth oxides [15], etc. were extensively investigated for water defluoridation. However, these materials have inherent drawbacks including low adsorption capacity, long time to achieve adsorption equilibrium, and poor regeneration possibility, restricting them to be applied in the purification of fluoride containing drinking water. There is also few investigation testing the possibility of adsorbent used in the purification of water to the allowable concentration of 1.5 mg/L for drinking. To overcome this challenge, an advance material design needs to be conducted, and an adsorbent with high affinity, adsorption capacity and fast kinetic for fluoride is urgent to be obtained.

Metal oxides tailored with functionalized polymers to change surface properties and improve the adsorption affinity for fluoride can be an advanced design. In recent days, more and more investigators pay their attention on polypyrrole (PPy) in adsorption due to its good environmental stability, non-toxic nature, good biocompatibility, relatively low cost and useful properties for adsorbent synthesis [16]. It was reported that PPy owns the excellent adsorption capacity for many contaminants through ion exchange or electrostatic interaction by novel positively charged nitrogen atoms in PPy matrix [16–18]. Moreover, PPy can undergo protonation or deprotonation process when it is treated with acid or alkali solution, resulting in doping or dedoping of counter ions. Owning to this reversible performance, adsorbents based on PPy can be easily regenerated [16]. For further improving the exposure of adsorption sites situated on PPy, the graft of PPy onto metal oxides have received extensive attention. Al_2O_3, SiO_2 and Fe_3O_4 modified with PPy were synthesized and evaluated for methylene blue (MB) removal, and the results showed that the adsorption capacity and affinity of PPy for MB were remarkably influenced and improved by metal oxides [16]. TiO_2 is also a good candidate used as a carrier in adsorbent tailoring thanks to its good stability, huge specific surface area and non-toxic nature [19]. Meanwhile, the hydroxyl groups attaching on the surface of TiO_2 makes it easy to be designed and modified [20]. Thus, TiO_2 modified with PPy would be a good design for the defluoridation from water.

In this study, TiO_2 modified with PPy was carefully designed and synthetized as a high affinity adsorbent to meet the acid test of defluoridation by *in-situ* chemical oxidative polymerization. FTIR, XRD, XPS, TG, N_2 isotherm analysis, SEM and Zeta potential analysis investigations were conducted to characterize surface and textural properties of the as-prepared PPy/TiO_2 composite. In order to apply composites in the defluoridation engineering of drinking water, the possibility was carefully estimated by adsorption isotherm and kinetic studies. Furthermore, the adsorption mechanism was extensively investigated and discussed by batch adsorption studies, including effect of pH, surface potential and thermodynamics.

2. Experimental section

2.1. Materials

Pyrrole (98%) purchased from Zhejiang Qingquan Pharmaceutical & Chemical Ltd, was distilled twice and stored in the dark under N_2 atmosphere. Other chemicals used in this study were of analytical reagent grades, and acquired from Sinopharm Chemical Reagent Co., Ltd (China). The deionized water was gained by EPED-40TF Superpure Water System (EPED, Nanjing).

2.2. Synthesis of PPy/TiO_2 composites

The PPy/TiO_2 composite was synthesized in the TiO_2 as-prepared suspension solution by *in-situ* chemical oxidative polymerization. Firstly, a mixture of *n*-propanol and tetrabutyl titanate with the volume ratio of 5:2 was carefully added into 200 mL of H_2SO_4 solution (0.24 mol/L), followed by being stirred for 24 h. Secondly, the formed as-prepared TiO_2 suspension solution was cooled to 5 °C in the dark, and then 0.675 mL of pyrrole monomer was dosed. After being stirred for 30 min, 25 mL of $FeCl_3$ solution (1.0 mol/L) was then added dropwise to the mixed solution and the solution was stirred for another 24 h. Finally, the PPy/TiO_2 composite was carefully filtrated and washed with the deionized water, and dried at 50 °C for 24 h under vacuum until the mass

became constant. For comparison, the pristine TiO_2 as-prepared was also synthesized with the same procedure without pyrrole monomer and $FeCl_3$ adding.

2.3. Characterization

The Fourier transform infrared (FTIR) spectra of PPy, TiO_2 and PPy/TiO_2 composite before and after adsorption were recorded in the range of 4000–400 cm^{-1} on a BRUKER TENSOR 37 FT-IR spectrometer by the KBr pellet method. X-ray diffraction (XRD) patterns were measured on an X'Pert PRO MRD Diffractometer by Cu-Kα radiation with wavelength of 1.5406 Å. The elements information were determined using X-ray photoelectron spectroscopy (XPS) on Kratos Axis Ultra DLD, with an Al monochromatic X-ray source (1486.71 eV), and all binding energies (BEs) were referenced to the C 1s hydrocarbon peak at 284.6 eV. The thermogravimetric (TG) analysis was measured on a Setaram Labsys Evo at a heating rate of 10 °C/min in N_2 flow. Textural properties including specific surface area, total pore volume and average pore radius were investigated at 77 K on a Builder SSA-4200 (China). The zeta potential investigation was conducted on a Malvern Zetasizer Nano ZS90.

2.4. Adsorption experiments

Standard fluoride solutions used in the study were prepared from anhydrous NaF with the deionized water. All samples were shaken in 20 mL F^- solution at an agitation speed of 200 rpm. Except co-existing ions, pretreatment and pH effect investigations, the adsorbents were pretreated with HNO_3 solution with pH = 1 to improve the adsorption capacity throughout this study. In order to obtain the optimized dosage, various dosages (0.5, 1, 1.5, 2, 2.5, 3 g/L) of PPy/TiO_2 composites were applied in 20 mg/L F^- solution at 25 °C. In the isotherm investigation, PPy/TiO_2 composites were added into various F^- initial concentrations of 10, 20, 40, 80, 100, 120, 150, 200 mg/L, and shaken at 25, 35, 45 °C, respectively for 3 h. For obtaining the kinetic data, the composites were suspended in the solutions with four F^- initial concentrations of 10, 20, 80, 150 mg/L, respectively in various contact time (0–180 min). To investigate the effect of co-existing ions, 20, 40, 60, 80 mg/L Cl^-, NO_3^-, HCO_3^-, SO_4^{2-}, CO_3^{2-}, and PO_4^{3-} ions were mixed with 20 mg/L F^- and applied in the study, respectively. In the mechanism investigation, the experiments were conducted at different pH (1–13) values with different pretreatment pH (1–13) values in 20 mg/L for 3 h, and the pH was adjusted using the HNO_3 and NaOH solution respectively. The pH before and after adsorption was recorded with a pH meter. In the thermodynamic study, 40 mg/L of F^- solution was applied and shaken at 25, 35, 40, 45 °C, respectively for 3 h. In the desorption study, 80 mg/L of F^- solutions were used to obtain saturated adsorbed adsorbents. 20 mL, 0.1 mol/L of NaOH were applied as elution agents for 60 min, and then 0.1 mol/L of HNO_3 was used as an active agent for another 60 min. Residual fluoride concentrations were determined by a fluoride-ion selective electrode using TISAB (PXSJ-216F, Leici, Shanghai) with careful correction. The adsorption capacity and removal rate were calculated according to equations as follows:

$$Q_e = \frac{(C_0 - C_e)V}{m}, \quad (1)$$

$$\text{Removal rate} = \frac{C_0 - C_e}{C_0} \times 100\%, \quad (2)$$

where Q_e (mg/g) is the equilibrium adsorption. C_0 and C_e (mg/L) are the F^- concentration at initial and equilibrium state, respectively. m (g) is the weight of adsorbent applied, and V (L) is the solution volume.

3. Results and discussion

3.1. Characterization of the PPy/TiO_2 composite

PPy was concluded to be non-toxic, good biocompatibility and strong combination to TiO_2 in our previous work [39]. The FTIR spectrum of the PPy/TiO_2 composite is shown in Fig. S1. For better comparison, the spectra of PPy as well as TiO_2 are also depicted. Their assignments are also listed in Table 1. Peaks demonstrated for pyrrole ring and TiO_2 can be found in the spectra, confirming the presence of PPy polymeric and TiO_2 compound. The peaks around 1188 cm^{-1} ascribed to the sulfate anion are also detected in the spectra of PPy/TiO_2, indicating that the sulfate anion was doped in PPy matrix, and the peak intensity can be used to suggest the doping level of the composite [21]. The FTIR spectra of the PPy/TiO_2 composite before and after F^- adsorption is shown in Fig. 1. It is interesting to be observed that the wavenumber of all peaks in terms of PPy are blue-shifted after F^- adsorption, and C—N, especially, is shifted from 1473 to 1482 cm^{-1}. And the peak situated at 1043 cm^{-1}, which indicates C—H in-plane bending vibration, disappears after adsorption. These can be explained that the skeletal vibration, which in terms of the delocalized π-electrons, is influenced by the doping ions of PPy after F^- adsorption [22]. This feature indicates that F^- is mainly attracted by PPy through electrostatic attraction and the positively charged nitrogen atoms play important roles in the adsorption [22]. A new peak situated in 848 cm^{-1}, which was also reported by Zhong et al. [23], and an additional peak at 530 cm^{-1} split from the TiO_2 band are also found in the spectrum after adsorption. These peaks demonstrate for Ti-F stretching vibration, indicating that F^- can be also adsorbed on the composite by replacing hydroxyls on TiO_2.

Table 1
The FT-IR absorptions in the region of 400–4000 cm^{-1} and their assignments.

Frequencies (cm^{-1})			Assignments
PPy	TiO_2	PPy/TiO_2	
1548	–	1543	C—C stretching vibration [39]
1473	–	1473	C—N stretching vibration [40]
1321	–	1310	C—H aromatic bending vibration [40,41]
–	1190	1191	Sulfate anion [1]
1047	–	1043	C—H in-plane bending vibration [42,43]
968	–	964	C—C out-plane bending vibration [38,39]
923	–	923	C—H out-plane bending vibration [40,41]
400–700	400–700	400–700	O—Ti—O [20,41]

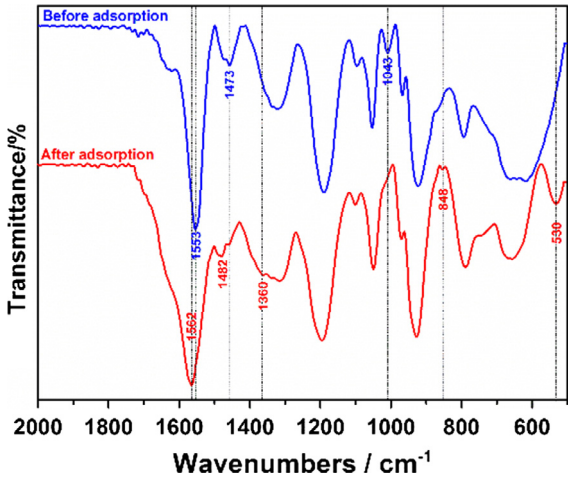

Fig. 1. FTIR spectra of the PPy/TiO_2 composite before and after adsorption with F^-.

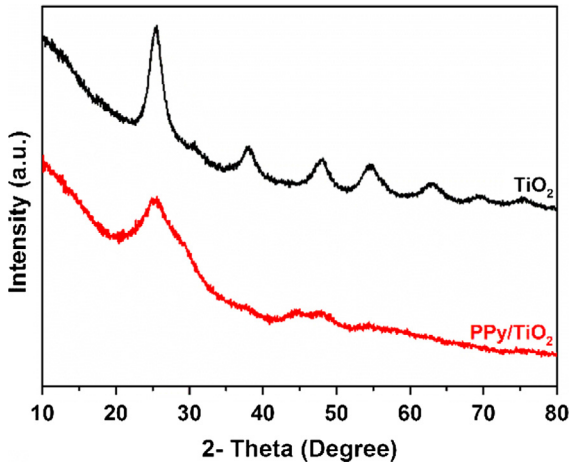

Fig. 2. XRD patterns of the as-prepared TiO_2 and PPy/TiO_2 composite.

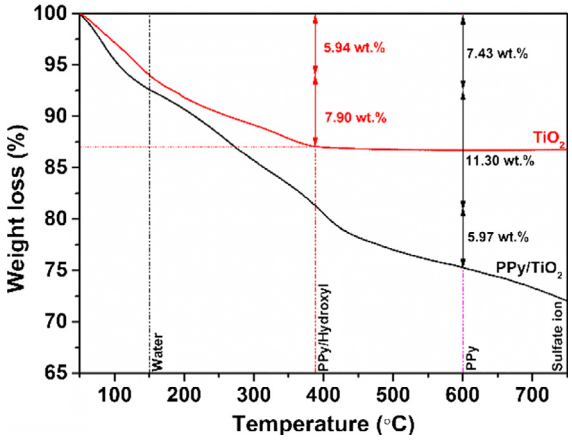

Fig. 4. TG analysis of the prepared TiO_2 and PPy /TiO_2 composite.

XRD patterns of the TiO_2 and PPy/TiO_2 are shown in Fig. 2. Main diffraction peaks at 25.3°, 37.8° and 48.1° are characteristic peaks of anatase TiO_2, confirming the existence of TiO_2 [21]. The degree of crystallinity becomes lower, and the intensity deceases after PPy modification, which may be due to the fact that PPy is mainly amorphous [16]. However, it is evident that peaks in the XRD patterns show no obvious difference between TiO_2 and PPy/TiO_2, indicating that the polymer only cover on the surface of TiO_2 without incorporating into TiO_2 layers [24].

To further demonstrate the presence of PPy and TiO_2, the XPS investigation is carefully conducted and shown in Fig. 3. Peaks assigned to O 1s, Ti 2p, N 1s, C 1s and S 2p are detected in the full scope spectrum of the PPy/TiO_2, confirming that the PPy/TiO_2 is successfully synthetized. Meanwhile, N 1s XPS spectra can be deconvoluted into two peaks at 399.9 and 401.3 eV which ascribed to neutral nitrogen atoms (NH) and positively charged nitrogen atoms (N^+) in the PPy layer, respectively, indicating the covalent-like binding between TiO_2 and PPy [25]. It should be noted that the positively charged nitrogen atom would result in more adsorption sites for F^-, followed by a higher adsorption capacity. The proportion of N^+ in the PPy modified is calculated to be 25% in terms of N^+/NH from the peak area [25].

The thermogravimetric analysis is applied to determine the content of PPy on the composite, and the result is shown in Fig. 4. To obtain the content of hydroxyls situated in TiO_2, the analysis of TiO_2 is also conducted. It shows that there is a three-stage process in the thermal degradation. The first weight loss, which is attributed to the loss of physically and chemically adsorb water, is calculated as 5.94 and 7.43 wt.% below 150 °C for TiO_2 and PPy/TiO_2, respectively [24]. The second weight loss interval is found to be between 150 and 600 °C, which is mainly ascribed to the thermal decomposition of hydroxyls for TiO_2 or hydroxyls and PPy for the composite, are about 7.90 and 17.27 wt.%, respectively [26]. Thus, PPy contents can be obtained through their difference values to be 9.37 wt.%. The final weight loss excess 600 °C in the analysis of PPy/TiO_2 is possibly due to the thermal decomposition of sulfate ions [21].

Textural properties of the PPy, TiO_2 and PPy/TiO_2 are investigated using N_2 isotherm study, and listed in Table 2. The specific surface area of the as-prepared PPy/TiO_2 reaches 95.71 m^2/g, showing a suitable specific surface area for adsorption sites exposure and benefits to F^- adsorption. It should be noted that its specific surface area is much lower than other adsorbents, showing the physical adsorption may not be a main adsorption mechanism in this case. Meanwhile, the specific surface area, total pore volume and average pore radius of TiO_2 reduce after modification with PPy, which is mainly due to the pore block of PPy [16]. SEM image shown in Fig. S2 confirms the spherical particle shape with agglomerated diameter of about 800 nm of PPy. Moreover, the cauliflower-like feature further indicates the formation of PPy on the surface of TiO_2 by comparison with the image of pure PPy [16].

Table 2
The textural properties of the TiO_2 and PPy/TiO_2 composite.

Composites	S_{BET} (m^2/g)	V (cm^3/g)	R (Å)
PPy	6.35	0.04	148.8
TiO_2	110.45	0.099	1.42
PPy/TiO_2	95.71	0.065	1.37

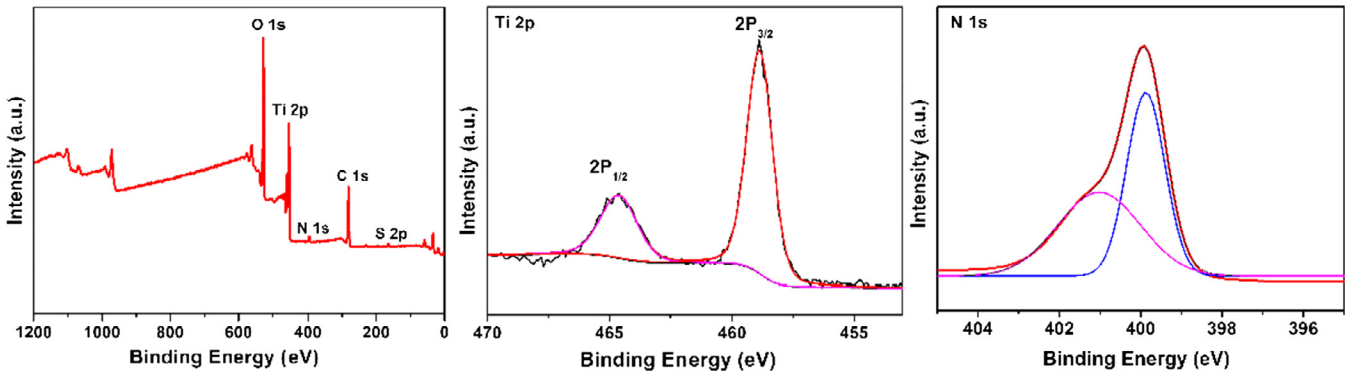

Fig. 3. XPS full scale and Ti 2p, N 1s core level spectra of the PPy/TiO_2 composite.

3.2. Adsorption investigations

3.2.1. Effect of dosage

The adsorbent dosage is vital for the cost in engineer. The effect of the composite dosage on F^- removal from the aqueous medium is depicted in Fig. 5. It is shown that the removal rate increases with the composite dosage due to abundant adsorption sites available at first stage, followed by an increase cease for the decrease of the adsorption driving force. The adsorption capacity also decreases as dosage increases due to the limit of adsorbates concentration [27]. Specifically, the removal rate increases from 58.8% at a dosage of 0.5–96.1% at a dosage of 3 g/L, reflecting that the amount of composite have a significant effect on the F^- adsorption. It is worthy to be noted that the adsorption capacity increases slightly when the dosage is larger than 2 g/L. To meet the water standard set by WHO, the 2 g/L of dosage was chosen as an optimized dosage.

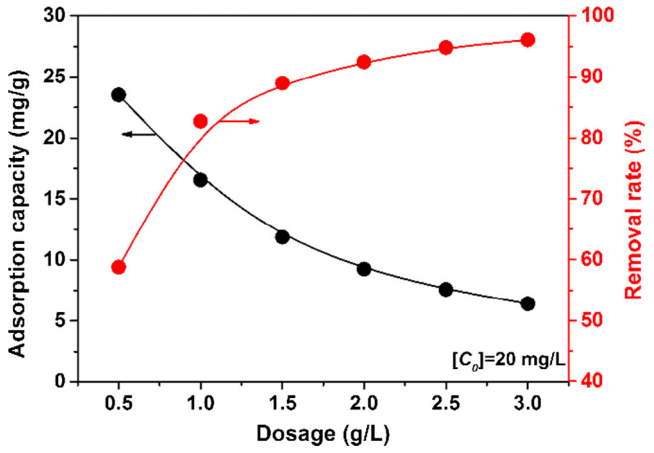

Fig. 5. Effect of adsorbent dosage on the adsorption capacity and removal efficiency of F^- onto the PPy/TiO_2 composite.

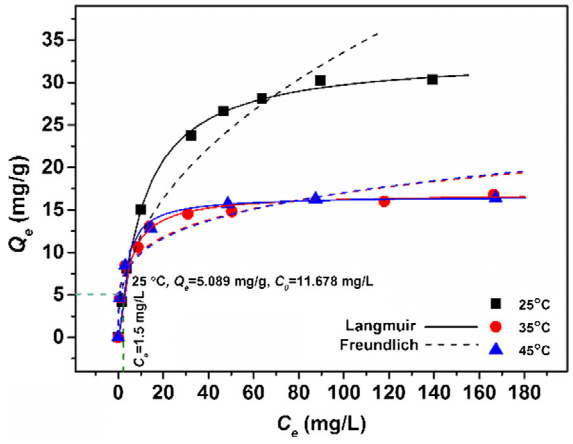

Fig. 6. Adsorption isotherms for F^- onto PPy/TiO_2 composite at various temperatures.

3.2.2. Adsorption isotherms

It's a prerequisite to obtain the adsorption isotherm to evaluate the adsorption capacity of composite and the possibility using it in the purification of fluoride containing water. Adsorption capacities at different F^- initial concentration at different temperature are shown in Fig. 6. Isotherms illustrate L-type, with a steep initial increase when the concentration is low, followed by a plateau for high concentration.

Data are described using Langmuir [28] and Frendlich [29] models to further obtain the information derived. Langmuir model can be given as the following equation:

$$Q_e = \frac{Q_m K_L Q_e}{1 + K_L Q_e} \tag{3}$$

where Q_m (mg/g) represents the maximum adsorption capacity, K_L (L/mg) is Langmuir constant relate to the affinity between the adsorbent and adsorbate. Meanwhile, the effect of equilibrium parameter R_L can be obtained as follows:

$$R_L = \frac{1}{1 + K_L C_0} \tag{4}$$

Data points are fitted to Langmuir model, and the corresponding parameters are listed in Table 3. It can be seen that points follow well with Langmuir model ($R^2 > 0.99$), including that the F^- adsorption onto the composite is monolayer, and adsorption sites distribute uniformly [30]. The maximum adsorption capacity reaches 33.178 mg/g at 25 °C, which is much larger than that of other composites (Table 4). The adsorption of F^- also deceases markedly as temperature increased, reflecting that the interaction between F^- and PPy/TiO_2 is exothermic. It's quite different from that obtained by Ensar Oguz [1], whose adsorbent shows temperature independence on F^- adsorption capacity. R_L acquired are all in the range of $0 < R_L < 1$, further confirming that the composite is favorable for F^- removal [31]. In order to evaluate the available of composite using for fluoride removal for drinking water to meet the WHO guideline value (1.5 mg/L), an operating line of C_e = 1.5 mg/L is used and shown in the Fig. 6. The initial solution

Table 4
Comparison of sorption capacities of various sorbents for F^-.

Adsorbent	Adsorption capacity (mg/g)	Ref.
Polyaniline	0.77	[44]
Activated carbon	2.50	[45]
Activated alumina	3.86	[45]
Carbon nanotubes	4.10	[46]
Nano-hydroxyapatite/chitosan	6.16	[47]
Polypyrrole	6.37	[18]
Al_2O_3/carbon nanotubes	14.90	[48]
Hydrous ferric oxide	16.50	[49]
Nanocrystalline TiO_2	25.31	[50]
Polypyrrole/TiO_2	33.17	This study

Table 3
Adsorption equilibrium parameters acquired from the Langmuir and Freundlich models in the adsorption of F^- onto the PPy/TiO_2 composite at various temperatures.

	Langmuir Model				Freundlich Model		
	Q_m (mg/g)	K_L (L/mg)	R_L	R^2	K_f ($mg^{1-n} \cdot L^n$/g)	1/n	R^2
25 °C	33.178	0.086	0.0549–0.538	0.999	7.291	0.447	0.932
35 °C	16.869	0.224	0.0218–0.446	0.998	6.089	0.224	0.955
45 °C	16.686	0.331	0.0149–0.232	0.999	5.790	0.235	0.960

concentration is calculated and predicted using obtained isotherms. If C_e = 1.5 mg/L, C_0 is calculated to be 11.678 mg/L. That is to say that even the initial concentration of F^- reaches 11.678 mg/L, the concentration of F^- in water can still be efficiently reduced below 1.5 mg/L after the adsorption of PPy/TiO_2 composite. It should be noted that the fluoride concentrations in the ground water of some village reach the highest of ~8 mg/L. In other words, PPy/TiO_2 could receive great novel to be used in the purification of fluoride containing ground water for drinking. Thus, PPy/TiO_2 shows outstanding affinity to fluoride than that of other adsorbents (Table 4).

Meanwhile, Freundlich model expressed as the following equation

$$Q_e = K_F C_e^{1/n} \quad (5)$$

which is also applied to depict the isotherm data, and the fitted parameters are also listed in Table 3. The fitted constant K_F, which is related to the adsorption capacity of adsorbent, is also reduced as the temperature increase, which is consistent with Langmuir results. However, the R^2 acquired is lower than that of Langmuir, further confirming that F^- adsorption on the composite is homogeneous.

3.2.3. Kinetics

Fig. 7 shows the excellent capability of PPy/TiO_2 to adsorb F^- in various initial concentration within different time. In order to meet the WHO guideline value for fluoride in drinking water, F^- containing water with initial concentration of 10 mg/L which obtained in isotherm study is also specifically investigated. Kinetics show mainly a two stages process that the adsorption capacity increase dramatically at the first stage, followed to be a constant after 60 min, showing a good affinity to F^- and the unique advance of PPy/TiO_2. The half-life of the process (t_{50}) also increases with the F^- initial concentration, confirming the rate of adsorption is initial concentration dependent. Nevertheless, it is still much shorter than that of other adsorbents. Moreover, when the composite is applied in the F^- containing water with the initial concentration of 10 mg/L (simulating the fluoride concentration in the high fluoride containing ground water of some village), the concentration of F^- is reduced less than 1.5 mg/L within 30 min. Thus, the composite shows a bright future to be used in the purification of fluoride containing water for drinking.

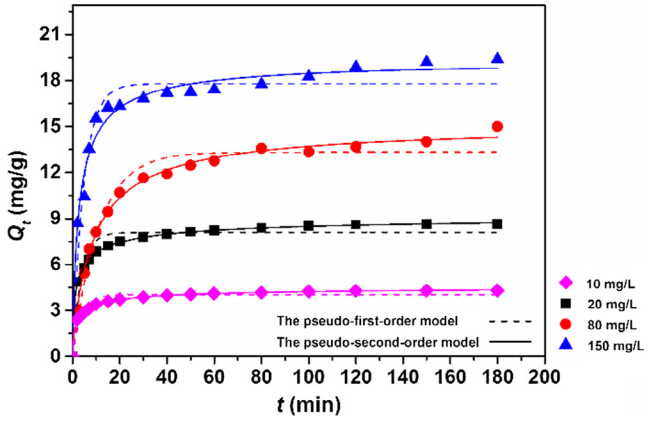

Fig. 7. Contact time versus the adsorption capacity of F^- onto PPy/TiO_2 composite at various initial concentrations.

Kinetic data are further described using the Lagergren first-order [32] and pesudo-second-order model [33]. The Lagergren first-order model which regarding that the adsorption is related to diffusion can be described as

$$Q_t = Q_e(1 - e^{-k_1 t}) \quad (6)$$

While the pesudo-second-order model which determines whether the adsorption process is controlled by chemisorption gives:

$$Q_t = \frac{Q_e^2 k_2 t}{1 + Q_e k_2 t} \quad (7)$$

where Q_e (mg/g) and Q_t (mg/g) are the adsorption amount at equilibrium state and at time t (min), respectively; k_1 (min^{-1}) and k_2 (g/(mg·min)) are the rate constants of two models, respectively. k_2 can be used to estimate the initial adsorption rate h (mg/(g·min)) as follows:

$$h = k_2 Q_e^2 \quad (t \to 0). \quad (8)$$

Fitting parameters are listed in Table 5, and typical lines are also depicted in Fig. 6. Data fit better to the pesudo-second-order model than the Lagergren first-order model, and predicted adsorption capacities are closer to the experimental one, revealing that the adsorption can be well described by the pesudo-second-order model, and the chemisorption involves in adsorption [34,35]. Furthermore, the initial adsorption rate h increases with initial concentrations due to the fact that the adsorption is a passive process using concentration gradient as a driving force. And it is novel that the initial adsorption rate is fast enough for drinking water purification when C_0 = 10 mg/L.

3.2.4. Influence of coexisting ions

Influence of coexisting ions such as chloride, nitrate, carbonate, sulfate, bicarbonate and phosphate ions in water on the F^- adsorption onto the as-prepared composite is conducted. Results are depicted in Fig. 8. It shows that the adsorption capacity, admittedly, dips with the ion charge increases. Nevertheless, the coexisting anions still have slight negative effect on F^- adsorption. This is because that the co-existing ions would compete for the same adsorption sites with F^-, and co-existing ions with more charge is more competitive. But the adsorbent has better affinity to F- than to other ions; as a consequence, F^- adsorption shows little drop under the competition of other ions. It should be noted that the effect of coexisting ions on F^- adsorption ability is slight even in the presence of phosphate with high concentration, showing a stable adsorption nature of PPy/TiO_2.

Table 5
Kinetic parameters obtained from the pseudo-first-order and pseudo-second-order models of F^- adsorption onto the PPy/TiO_2 composite at various initial concentrations.

C_0 (mg/L)	$Q_{e,exp}$ (mg/g)	The pseudo-first-order model			The pseudo-second-order model			
		K_1 (1/min)	$Q_{e,1}$ (mg/g)	R^2	K_2 (g·min/mg)	h (mg/(g·min))	$Q_{e,2}$ (mg/g)	R^2
10	4.29	0.283	4.05	0.808	0.039	0.752	4.39	0.998
20	8.70	0.273	8.09	0.708	0.036	2.775	8.78	0.999
80	15.25	0.091	13.33	0.949	0.013	2.996	15.18	0.997
150	19.55	0.021	17.79	0.859	0.011	4.213	19.57	0.999

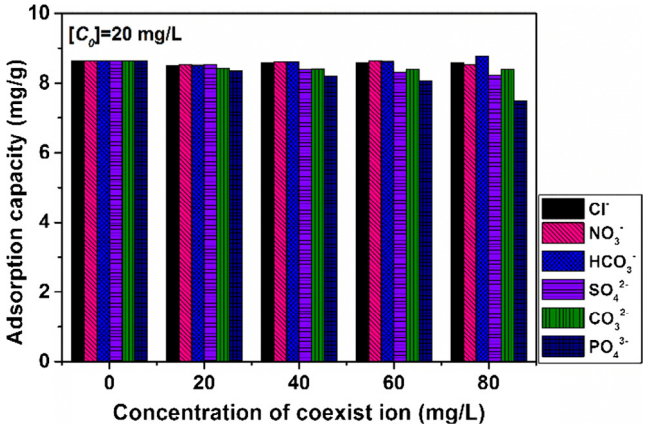

Fig. 8. Effect of various concentrations of co-exist ions on the adsorption of F^- onto PPy/TiO_2 composite.

3.3. Adsorption mechanism

3.3.1. Effect of initial pH

Adsorption characteristics are strongly influenced by the initial pH of the water. Thus, the composite is exposed under pH range from 1 to 13 to optimize the adsorption process and understand the adsorption mechanism. Results illustrated in Fig. 9 shows that the adsorption capacity increases with pH when pH < 7, and reduces after that. Such a trend was also reported in other adsorption system [1]. Generally, the composite surface is hydroxylated in the aqueous solution. The hydroxylated surface and the hydroxyl composite would develop charge and adsorption sties for F^- adsorption. It is acknowledged that F^- could be specifically adsorbed on the composite through ionic exchange as follows if the adsorption is pH-dependent [36]:

$$\text{Composite-OH} + H^+ \leftrightarrow \text{Composite-OH}_2^+ \quad (9)$$

$$\text{Composite-OH}_2^+ + F^- \leftrightarrow \text{Composite-OH}_2 - F \quad (10)$$

$$\text{Composite-OH}_2^+ + F^- \leftrightarrow \text{Composite-F} + H_2O \quad (11)$$

$$2[\text{Composite-OH}] + 2F^- + 2H^+ \leftrightarrow 2\text{Composite-OF}^{2-} + 4H^+ \rightarrow 2\text{Composite-F} + 2H_2O \quad (12)$$

The ionic exchange process is confirmed by pH changes after adsorption. The data shown in Table S1 indicate that a certain number of hydroxyls were released after the F^- adsorption, resulting from the ionic exchange process. This is specifically in accordance with the results obtained in FTIR. The adsorption is found to be unfavorable in the acid condition, which is attributed to the formation of hydrofluoric acid with weak ionization [1]. Meanwhile, the adsorption capacity is low at alkaline range, and this is due to the competition with OH^-. The optimized pH is around 7, which falls into the pH range of drinking water, showing a suitability to apply the composite in drinking water defluoridation.

To further investigate the stable adsorption nature of PPy/TiO_2 as-prepared and reduce the treatment cost, the recycle strategy is proposed. Considering that F^- is hard to be adsorbed on the composite at pH = 13, 0.1 mol/L NaOH is applied as a desorption agent. Recycle results depicted in Fig. 10 show a good stability after six cycles, and the adsorption capacity even improves in the second cycle. This may be due to the dislodging of impurities in the pore after alkaline treatment [20]. The near 100 percent regeneration of the composite sorbent at room temperature for so many adsorption cycles further confirm the primary physical nature of adsorption such as ionic exchange for fluoride onto the composite adsorbent. Results make the composite more attractive in drinking water defluoridation engineering for its low treatment cost and high removal efficiency.

3.3.2. Effect of surface potential

For the further investigation on the surface potential, the zeta potential study is carefully carried out. The pH of zero point charge (pH_{pzpc}) is obtained as 10.3 (Fig. 11), showing a unique affinity for

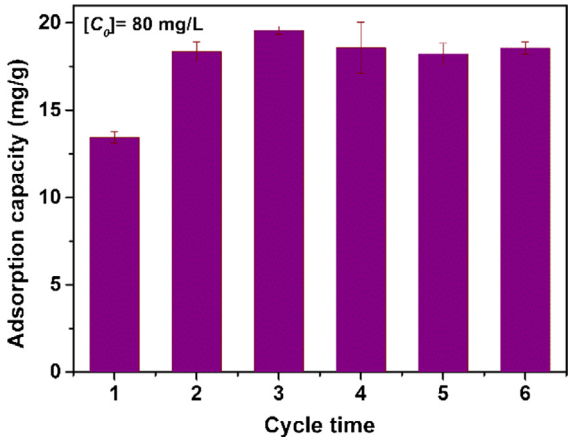

Fig. 10. Adsorption recycle stabilities of the PPy/TiO_2 composite for F^- adsorption.

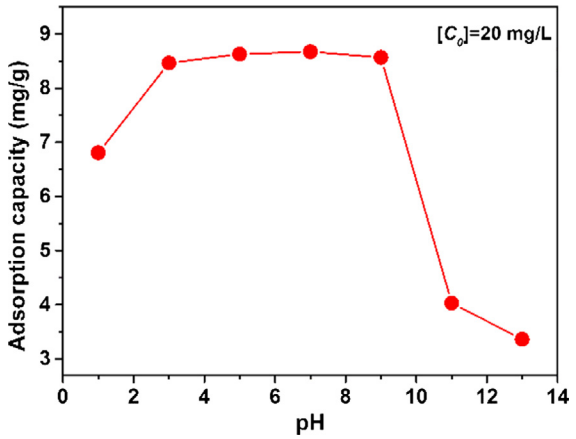

Fig. 9. Effect of solution pH on the adsorption capacity of the PPy/TiO_2 composite for F^-.

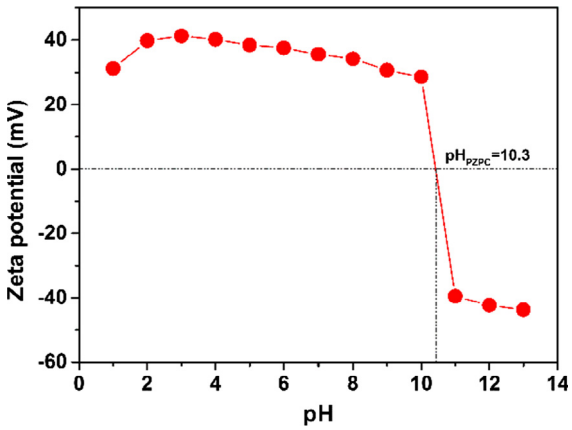

Fig. 11. Zeta potentials of the PPy/TiO_2 composite.

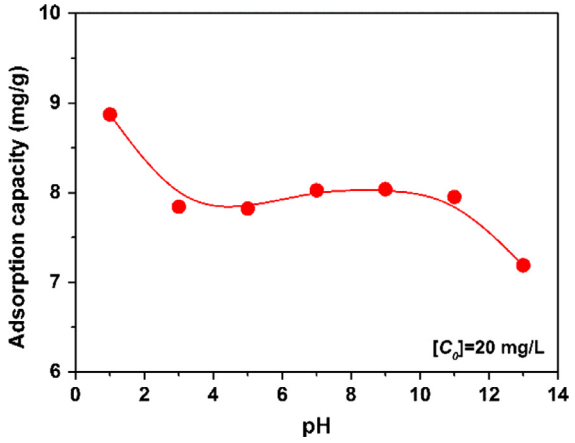

Fig. 12. Effect of surface potentials on the adsorption capacity of the PPy/TiO_2 composite for F^-.

F^- adsorption through electrostatic attraction due to the positive charge on the surface in wide pH range. The effect of surface potential on the adsorption capacity is shown in Fig. 12. The adsorption capacity of the composite decreases with the pH of the pretreatment solution, and the maximum adsorption capacity at pH = 1 of the pretreatment solution is noticed. Literatures [16,37] pointed out that some charges may be carried on the surface of PPy when composites were pretreated in a solution through the following equations:

$$PPyX + H^+ \leftrightarrow PPyXH^+ \quad (pH < pH_{pzpc}) \tag{13}$$

$$PPyX + OH^- \leftrightarrow PPyXOH^- \quad (pH > pH_{pzpc}) \tag{14}$$

where X is the counter anions. Moreover, the nitrogen atom situated on the PPy matrix could still be positive charged. It can be noticed that the adsorption capacity begins to decrease at pH > 10, which consists well with the pH_{pzpc} (10.3), stating that the electrostatic attraction may play an important role in F^- adsorption. It should be noted that the adsorption capacity is still high with pretreatment of pH = 7 solution, confirming that the composite could be safely applied in the drinking water purification without changing the pH of water.

3.3.3. Thermodynamics

The thermodynamics investigation is carried out to study the mechanism of the adsorption behavior under various temperature. Thermodynamic parameters including enthalpy (ΔH^0/kJ·mol^{-1}), Gibbs free energy (ΔG^0/kJ·mol^{-1}) and entropy (ΔS^0/J·K^{-1}·mol^{-1}) could be acquired from thermodynamic equations as follows:

$$\Delta G^\circ = \Delta H^\circ - T\Delta S^\circ = -RT \ln K_T \tag{15}$$

$$\ln K_T = \frac{\Delta S^\circ}{R} - \frac{\Delta H^\circ}{RT} \tag{16}$$

where R (J/(mol·K) is the gas constant equaling 8.314; K_T (L/mg) referred to adsorption affinity could be determined by $(C_0 - C_e)/C_e$. The plot of $\ln K_T$ versus 1/T is depicted in Fig. S3, and fitting results are listed in Table 6. The enthalpy (ΔH^0) is negative, revealing that the adsorption favors in low temperature, which is in according with the result of isotherm investigation. The entropy (ΔS°) shows a negative value, stating that the adsorption is a randomness-decrease process. While negative values of Gibbs free energy indicate that the adsorption is a spontaneous process. Values of Gibbs free energy could be applied to describe the adsorption mechanism: (1) The adsorption is mainly physical when the value is between −20 and 0 kJ/mol, (2) the joint action of physical sorption and chemisorption in −20 to −80 kJ/mol, (3) chemisorption in the range of −80 to −400 kJ/mol. The values of Gibbs free energy in this study acquired range from 0 to −3 kJ/mol, further confirming that electrostatic attraction may occupy important roles in the adsorption [38].

Table 6
Thermodynamic parameters of F^- adsorption onto the PPy/TiO_2 composites

ΔH (kJ/mol)	ΔS (J/(K·mol))	T (K)	ΔG (kJ/mol)
−21.393	−62.804	25 °C	−2.741
		35 °C	−1.851
		45 °C	−1.400

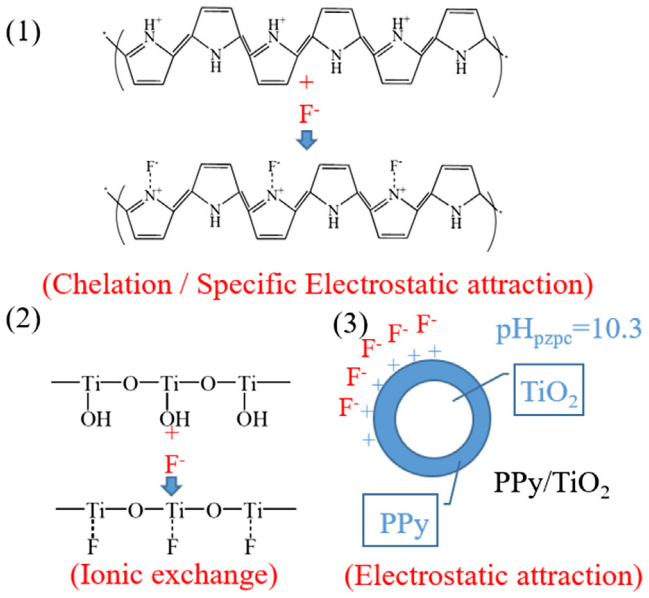

Scheme 1. The possible mechanism for the adsorption of F^- onto PPy/TiO_2 composite from aqueous medium.

Taking all the results discussed above into consideration, F^- could be specifically adsorbed on the composite through ionic exchange by replacing hydroxyl or H_2O situated in the hydroxylated surface on the composite, but it is not the prominent adsorption mechanism according to the Gibbs free energy (from 0 to −3 kJ/mol). Furthermore, the pretreatment with low pH solution could improve the F^- adsorption due to electrostatic attraction with the positive charged composite and this mechanism may be the major cause for F^- adsorption. It could not be neglected that the adsorption rate is controlled by chemisorption from the kinetics study, and it can be deduced that the nitrogen atoms situated on the PPy matrix could play a role of specific adsorption sites to chelate with F^-. Thus, chelation may be also involved, even though insignificant, in the adsorption. The plausible F^- adsorption mechanism of the PPy/TiO_2 is evidently proposed and shown in Scheme.1.

4. Conclusions

Herein, a high efficiency and affinity defluoridation adsorbent PPy/TiO_2 composite was carefully designed and synthetized by *in-situ* chemical oxidative polymerization. And the low-cost and novel adsorbent is confirmed that it can be applied in the purification of fluoride containing water for drinking. Surface and textural characterizations and abundant positively charged nitrogen atoms (N^+) show a suitability for fluoride adsorption by composite. The maximum monolayer adsorption capacity reaches 33.178 mg/g at

25 °C, nearly fifty-five times more than the adsorption capacity of PANI, fivefold that of PPy, and twice the amount of hydrous ferric oxide. The concentration of F^- containing water after adsorption can be reduced below 1.5 mg/L within 30 min for drinking water at pH of 7 even its initial concentration reached 11.678 mg/L. The adsorption can be well described by the pesudo-second-order model, revealing that the chemisorption is involved in the adsorption. The initial adsorption rate *h* is also found to increase with the initial concentrations. Moreover, the adsorbent can be easily recycled without adsorption capacity loss after six cycles, greatly confirming the outstanding affinity to fluoride. The adsorption is confirmed to be a spontaneous and exothermic process with decreasing entropy, which is prominently conducted through electrostatic attraction, ionic exchange, and chelation may be also involved. The detailed information about using the adsorbent to treat the real wastewater containing F^- is projected to be conducted in our future work.

Acknowledgements

The authors gratefully acknowledge the financial supports from the National Natural Science Foundation of China (Grant No. 21307098), and Jingjing Li for her kindly work and advice.

Appendix A. Supplementary material

Supplementary data associated with this article can be found, in the online version, at http://dx.doi.org/10.1016/j.jcis.2017.01.084.

References

[1] E. Oguz, Adsorption of fluoride on gas concrete materials, J. Hazard. Mater. 117 (2005) 227–233.
[2] Y. Wang, E.J. Reardon, Activation and regeneration of a soil sorbent for defluoridation of drinking water, Appl. Geochem. 16 (2001) 531–539.
[3] H. Lounici, L. Addour, D. Belhocine, H. Grib, S. Nicolas, B. Bariou, N. Mameri, Study of a new technique for fluoride removal from water, Desalination 114 (1997) 241–251.
[4] H. Sadallah, Guidelines for Drinking-water Quality, 3rd ed., 2006, World Health Organization, 2015.
[5] B.K. Handa, Geochemistry and genesis of fluoride-containing ground waters in India, Ground Water 13 (1975) 275–281.
[6] J. Cheng, X. Meng, C. Jing, J. Hao, La^{3+}-modified activated alumina for fluoride removal from water, J. Hazard. Mater. 278 (2014) 343–349.
[7] Drinking Water Atlas of China, China Cartographic Publishing House, 1991.
[8] M.S. Onyango, Y. Kojima, O. Aoyi, E.C. Bernardo, H. Matsuda, Adsorption equilibrium modeling and solution chemistry dependence of fluoride removal from water by trivalent-cation-exchanged zeolite F-9, J. Colloid Interface Sci. 279 (2004) 341–350.
[9] G. Singh, J. Majumdar, Removal of fluoride from spent pot liner leachate using ion exchange, Water Environ. Res. 71 (1998) 36–42.
[10] S.K. Adhikary, U.K. Tipnis, W.P. Harkare, K.P. Govindan, Defluoridation during desalination of brackish water by electrodialysis, Desalination 71 (1989) 301–312.
[11] R. Simons, Trace element removal from ash dam waters by nanofiltration and diffusion dialysis, Desalination 89 (1993) 325–341.
[12] N. Parthasarathy, J. Buffle, W. Haerdi, Combined use of calcium salts and polymeric aluminium hydroxide for defluoridation of waste waters, Water Res. 20 (1986) 443–448.
[13] M. Islam, R.K. Patel, Evaluation of removal efficiency of fluoride from aqueous solution using quick lime, J. Hazard. Mater. 143 (2007) 303–310.
[14] M. Srimurali, A. Pragathi, J. Karthikeyan, A study on removal of fluorides from drinking water by adsorption onto low-cost materials, Environ. Pollut. 99 (1998) 285–289.
[15] A.M. Raichur, M.J. Basu, Adsorption of fluoride onto mixed rare earth oxides, Sep. Purif. Technol. 24 (2001) 121–127.
[16] J. Chen, J. Feng, W. Yan, Influence of metal oxides on the adsorption characteristics of PPy/metal oxides for Methylene Blue, J. Colloid Interface Sci. 475 (2016) 26–35.
[17] M.L. Zhang, H.Y. Zhang, D. Xu, L. Han, D.X. Niu, B.H. Tian, J.A. Zhang, L.Y. Zhang, W.S. Wu, Removal of ammonium from aqueous solutions using zeolite synthesized from fly ash by a fusion method, Desalination 271 (2011) 111–121.
[18] M. Karthikeyan, K.K. Satheeshkumar, K.P. Elango, Removal of fluoride ions from aqueous solution by conducting polypyrrole, J. Hazard. Mater. 167 (2009) 300–305.
[19] M. Janus, E. Kusiak, J. Choina, J. Ziebro, A.W. Morawski, Enhanced adsorption of two azo dyes produced by carbon modification of TiO_2, Desalination 249 (2009) 359–363.
[20] J. Chen, J. Feng, W. Yan, Facile synthesis of a polythiophene/TiO_2 particle composite in aqueous medium and its adsorption performance for Pb(ii), RSC Adv. 5 (2015) 86945–86953.
[21] Z.-C. Wang, H.-F. Shui, Effect of PO_4^{3-} and PO_4^{3-}–SO_4^{2-} modification of TiO_2 on its photocatalytic properties, J. Mol. Catal. A: Chem. 263 (2007) 20–25.
[22] M. Bhaumik, T.Y. Leswifi, A. Maity, V.V. Srinivasu, M.S. Onyango, Removal of fluoride from aqueous solution by polypyrrole/Fe_3O_4 magnetic nanocomposite, J. Hazard. Mater. 186 (2011) 150–159.
[23] Y.H. Zhong, Q. Zhou, J.Q. Liu, Y. Wang, X. Chen, Y.C. Wu, Preparation of fluorizated TiO_2 hollow microspheres and their photocatalytic activity, Chin. J. Inorg. Chem. 29 (2013) 2133–2139.
[24] J. Xu, P. Yao, X. Li, F. He, Synthesis and characterization of water-soluble and conducting sulfonated polyaniline/para-phenylenediamine-functionalized multi-walled carbon nanotubes nano-composite, Mater. Sci. Eng. B – Adv. Funct. Solid-State Mater. 151 (2008) 210–219.
[25] E.T. Kang, K.G. Neoh, Y.K. Ong, K.L. Tan, B.T.G. Tan, X-ray photoelectron spectroscopic studies of polypyrrole synthesized with oxidative Fe(III) salts, Macromolecules 24 (1991) 2822–2828.
[26] K. Nagaveni, G. Sivalingam, M.S. Hegde, G. Madras, Solar photocatalytic degradation of dyes: high activity of combustion synthesized nano TiO_2, Appl. Catal. B 48 (2004) 83–93.
[27] Y.S. Ho, Second-order kinetic model for the sorption of cadmium onto tree fern: a comparison of linear and non-linear methods, Water Res. 40 (2006) 119–125.
[28] I. Langmuir, The adsorption of gases on plane surface of glass, mica and platium, J. Am. Chem. Soc. 40 (1918) 1361–1403.
[29] H. Freundlich, Concerning adsorption in solutions, Zeitschrift Fur Physikalische Chemie-Stochiometrie Und Verwandtschaftslehre 57 (1906) 385–470.
[30] A.H. Chen, S.C. Liu, C.Y. Chen, C.Y. Chen, Comparative adsorption of Cu(II), Zn (II), and Pb(II) ions in aqueous solution on the crosslinked chitosan with epichlorohydrin, J. Hazard. Mater. 154 (2008) 184–191.
[31] A. Kurniawan, H. Sutiono, N. Indraswati, S. Ismadji, Removal of basic dyes in binary system by adsorption using rarasaponin–bentonite: revisited of extended Langmuir model, Chem. Eng. J. 189–190 (2012) 264–274.
[32] S. Lagergren, About the theory of so-called adsorption of solution substances, 1998.
[33] Y.S. Ho, G. McKay, Pseudo-second order model for sorption processes, Process Biochem. 34 (1999) 451–465.
[34] Y.S. Ho, G. McKay, Sorption of dye from aqueous solution by peat, Chem. Eng. J. 70 (1998) 115–124.
[35] Y.S. Ho, Review of second-order models for adsorption systems, J. Hazard. Mater. 136 (2006) 681–689.
[36] R. Weerasooriya, H.U.S. Wickramarathne, H.A. Dharmagunawardhane, Surface complexation modeling of fluoride adsorption onto kaolinite, Colloids Surf. A 144 (1998) 267–273.
[37] X. Zhang, R. Bai, Adsorption behavior of humic acid onto polypyrrole-coated nylon 6,6 granules, J. Mater. Chem. 12 (2002) 2733–2739.
[38] G.D. Vuković, A.D. Marinković, S.D. Škapin, M.Đ. Ristić, R. Aleksić, A.A. Perić-Grujić, P.S. Uskoković, Removal of lead from water by amino modified multi-walled carbon nanotubes, Chem. Eng. J. 173 (2011) 855–865.
[39] N.V. Blinova, J. Stejskal, M. Trchova, J. Prokes, M. Omastova, Polyaniline and polypyrrole: a comparative study of the preparation, Eur. Polym. J. 43 (2007) 2331–2341.
[40] X.M. Feng, Z.Z. Sun, W.H. Hou, J.J. Zhu, Synthesis of functional polypyrrole/prussian blue and polypyrrole/Ag composite microtubes by using a reactive template, Nanotechnology 18 (2007) 7.
[41] J. Li, Q. Zhang, J. Feng, W. Yan, Synthesis of PPy-modified TiO_2 composite in H_2SO_4 solution and its novel adsorption characteristics for organic dyes, Chem. Eng. J. 225 (2013) 766–775.
[42] A. Uygun, A.G. Yavuz, S. Sen, M. Omastová, Polythiophene/SiO_2 nanocomposites prepared in the presence of surfactants and their application to glucose biosensing, Synth. Met. 159 (2009) 2022–2028.
[43] Q. Lu, Y. Zhou, Synthesis of mesoporous polythiophene/MnO_2 nanocomposite and its enhanced pseudocapacitive properties, J. Power Sources 196 (2011) 4088–4094.
[44] M. Karthikeyan, K.K. Satheeshkumar, K.P. Elango, Defluoridation of water via doping of polyanilines, J. Hazard. Mater. 163 (2009) 1026–1032.
[45] R.L. Ramos, J. Ovalle-Turrubiartes, M.A. Sanchez-Castillo, Adsorption of fluoride from aqueous solution on aluminum-impregnated carbon, Carbon 37 (1999) 609–617.
[46] Y.H. Li, S. Wang, X. Zhang, J. Wei, C. Xu, Z. Luan, D. Wu, Adsorption of fluoride from water by aligned carbon nanotubes, Mater. Res. Bull. 38 (2003) 469–476.
[47] C.S. Sundarama, Uptake of fluoride by nano-hydroxyapatite/chitosan, a bioinorganic composite, Bioresour. Technol. 99 (2008) 8226–8230.
[48] Y.H. Li, S. Wang, A. Cao, Z. Dan, X. Zhang, C. Xu, Z. Luan, D. Ruan, L. Ji, D. Wu, Adsorption of fluoride from water by amorphous alumina supported on carbon nanotubes, Chem. Phys. Lett. 350 (2001) 412–416.
[49] S. Dey, S. Goswami, U.C. Ghosh, Hydrous ferric oxide (HFO)—a scavenger for fluoride from contaminated water, Water Air Soil Pollut. 158 (2004) 311–323.
[50] H. Deng, Adsorption performance of nanocrystalline TiO_2 to fluoride ions, Ind. Water Wastewater 4 (2013) 17–20.